

## **CHAPTER – 8**

### **METAMORPHIC CONDITION**

*"Geology is the study of pressure and time. That's all it takes really, pressure, and time."*  
Morgan Freeman

#### **8.1 Introduction**

An estimate of PT condition is a challenging exercise for the rocks because it underwent different metamorphism episodes. The mineral compositions are not free from re-equilibration during cooling, which affects the peak composition by cation exchanges. It is established that the mineral compositions in natural rocks are difficult to interpret and expected to get the 'preserve equilibrium distributions' of all elements of concern from peak conditions. This 'difficult-to-quantify' compositional variability affects both the precision and accuracy of thermobarometry approaches more seriously than the mineral assemblage (petrogenetic grid) approach.

In this chapter, an attempt has been made to discuss the paragenesis and phase relations of different mineral assemblages of the coexisting mineral phases at varying P-T conditions based on the mineral composition data, along with geothermobarometry and bulk composition modelling of the rock of high-grade gneisses, pelitic granulites and mafic granulites.

#### **PART – A: Phase Petrology**

##### **8.A.1 Introduction**

The study of various mineral parageneses is generally supported by graphical projections in the pertinent system, known as a phase diagram. These chemographic projections provide an easy tool for understanding the phase compatibility relationships

and deducing metamorphic reactions in forming diverse mineral assemblages. Phase relationship and the analyses of coexisting minerals in a pertinent system will provide the data which indicates equilibrium crystallization or any disappearance from chemical equilibrium. If minerals coexist in a rock crystallized in equilibrium, the distribution of elements amongst the minerals could be systematic. The petrogenetic grid has univariant reaction lines that bounded all possible divariant mineral assemblages' fields for a given bulk chemical composition. The univariant reactions curves delineating the stability limit of many end-members mineral equilibrium have been studied experimentally. As more thermodynamic data become available, it will be easier to calculate the stability of minerals theoretically, and this will be probably the main thrust in future studies of metamorphic mineral assemblages.

## **8.A.2 Phase compatibility relation**

### **8.A.2.1 High-grade gneiss**

The high-grade gneisses are plotted in FeO-MgO-Al<sub>2</sub>O<sub>3</sub>-SiO<sub>2</sub>-H<sub>2</sub>O (FMASH) system in AFM projection diagram (Fig.8.1). Mineral parageneses are result from the reaction between garnet and gedrite reflect the stability of garnet-cordierite-gedrite. The mineral association is a poly-metamorphism product and is an association of mineral assemblages of different metamorphic stages. The following metamorphic reactions support these:

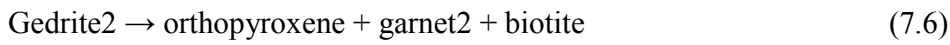
Early-stage: Prograde reaction:



Middle stage: Prograde reaction:



Peak stage:



Retrograde stage:

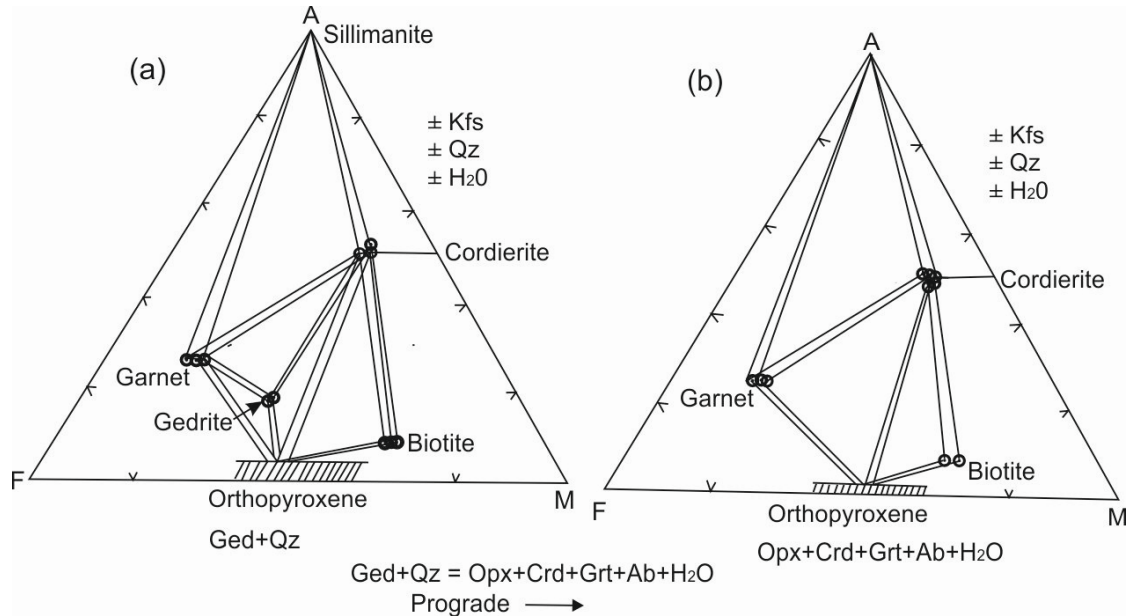
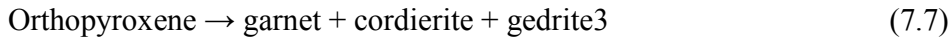


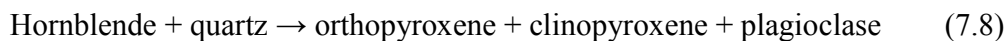
**Figure 8.1** AFM projection from K-feldspar point of the AKFM tetrahedron onto the AFM plane: (a) Showing the gedrite in the middle of triangle Grt–Crd–Opx in which gedrite is reactant; (b) Depicts the disappearance of gedrite to form the triangle Grt–Crd–Opx as a product, where  $A = \text{Al}_2\text{O}_3 + \text{Fe}_2\text{O}_3 - (\text{K}_2\text{O} + \text{Na}_2\text{O} + \text{CaO})$ ;  $F = \text{FeO} + \text{MnO}$ ;  $M = \text{MgO}$ .

The three-phase field of garnet-gedrite-biotite from the AKF diagram suggests that the cordierite-garnet-biotite field was terminated with new assemblages of cordierite–gedrite–biotite according to reaction (7.2). Reaction (7.2) in the given form has been studied at low pressure by [413]. According to [414], biotite with higher  $X_{\text{Mg}}$  used by [413] would also produce cordierite at higher pressures. However, it is evident from the petrogenetic grid of [415], the assemblages gedrite-cordierite-garnet-K-feldspar may be found in two condition, high pressure/ high temperature and relatively low pressure/ low temperature of his diagram. In the three-phase field of gedrite-orthopyroxene-garnet and

gedrite–cordierite–garnet (Fig.8.1), orthopyroxene appears from reaction (7.6) and can be represented by the phase compatibility diagram change from Figures 8.1a&b.

### 8.A.2.2 Mafic granulites

The phase relationships of the mafic granulite have been discussed in the model system of CaO-(MgO+FeO)-Al<sub>2</sub>O<sub>3</sub>-SiO<sub>2</sub>-H<sub>2</sub>O and first investigated graphically in the ACF diagram (Fig.8.2), with the components of this subsystem suitably represent the coexisting opx, cpx, hbl, and plg. Na<sub>2</sub>O is a significant amount in plagioclase and hornblende, whereas FeO and TiO<sub>2</sub> are common in hornblende. Biotite and k-feldspar occur as the limited amount may be due to non-availability of K<sub>2</sub>O, so K<sub>2</sub>O has neglected for graphical representation. In particular, the orthopyroxene-clinopyroxene-plagioclase mineral assemblage (Fig.8.2) occurs in response to the hornblende break down, forming a three-phase field by breaking the tie lines hornblende-plagioclase, hornblende-clinopyroxene, and hornblende-orthopyroxene through the reaction (7.8). This reaction (7.8) is a continuous reaction that primarily depends on quartz's availability for the complete breakdown hornblende. Indeed, the Daltonganj mafic granulites commonly consist the mineral assemblage; orthopyroxene-clinopyroxene-hornblende-plagioclase-biotite-ilmenite-quartz, depending upon the availability of quartz. Several metamorphic reactions have been observed in mafic granulites, in which a textural relation shows corroded hornblende is present as inclusion in the pyroxene. The reaction is;



The reaction is derived from the ACF diagram (Fig.8.3). The hornblende breaks down to form three-phase clinopyroxene-orthopyroxene-plagioclase. The Ti has strongly

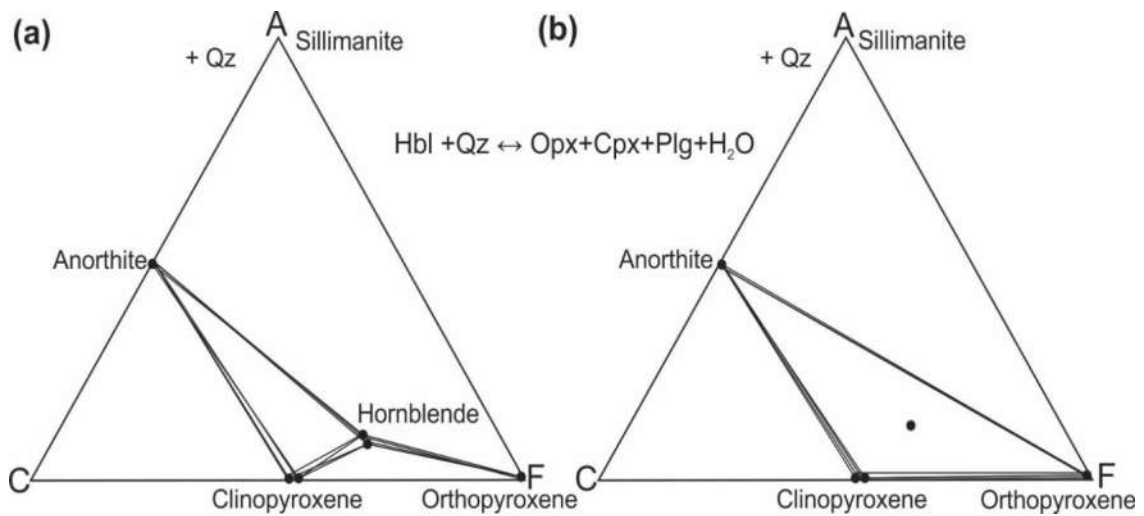


**Figure 8.2**(a) The observed mineral assemblages (solid circle) of the mafic granulites are shown in the ACF diagram. (b) The mineral assemblage orthopyroxene-clinopyroxene-plagioclase is formed due to the hornblende tie line's consumption during a prograde reaction.

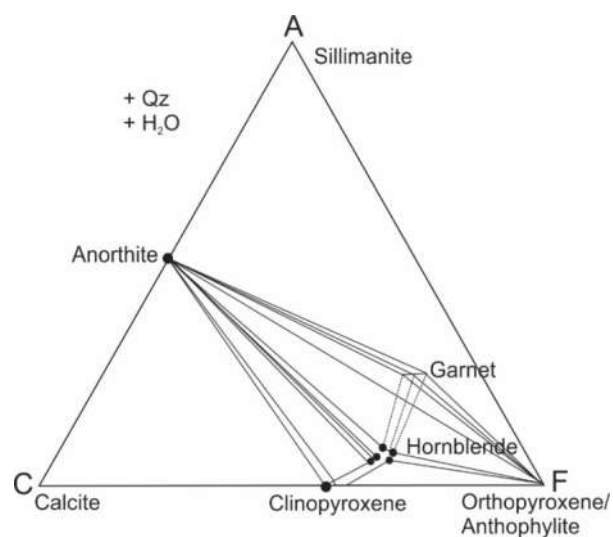
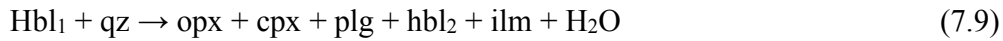


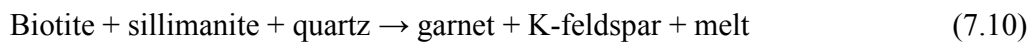
**Figure 8.3** The mineral composition of the mafic granulites are shown in ACF diagram where, A =  $(Al_2O_3 + Fe_2O_3) - (K_2O + Na_2O)$ ; C = CaO; F = FeO + MgO + MnO. ( $A+C+F = 100$  mol%)

partitioned in hornblende comparison to pyroxene due to a decrease in a modal constituent that causes the enrichment of Ti in hornblende. Besides, hornblende can be completely used to repel ilmenite granules commonly found adjacent to corroded hornblende. Thus, continuation reaction is:



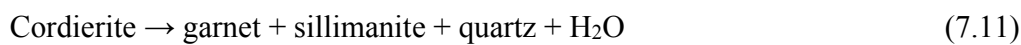
### 8.A.2.3 Pelitic granulites

The four-phase assemblage has less variance, and thus the composition of the phases should be uniquely defined if the rocks have equilibrated at similar pressure and temperature. The three-phase fields of garnet-cordierite-sillimanite and garnet-cordierite-biotite exhibit different FeO/MgO ratio suggesting different externally controlled extensive variables during their crystallization. The Fe-Mg cation exchange among garnet and biotite, evident from the compositional element, suggests crystallization near the thermal peak of metamorphism followed by cooling during which cation exchange reactions continued. In pelitic granulites, the garnet is formed through the reaction;

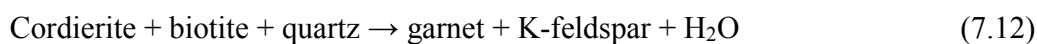


Here, one three-phase field of garnet-biotite-sillimanite and it is evident from biotite-sillimanite join intersected by garnet-K-feldspar joins in the AKF diagram (Fig.8.4). The textural feature such as linear trails of biotite and coarse needle of sillimanite within a garnet document, the evidence is favouring the reaction (7.10).

The continuous Fe-Mg reactions in the three-phase field of garnet-cordierite-sillimanite may be given as:



And for the three-phase field of garnet-cordierite-biotite



Both (7.11 and 7.12) are continuous Fe-Mg reactions. The relative  $X_{\text{Mg}}$  in the phases concerned here:  $\text{Crd} > \text{Bt} > \text{Grt core} > \text{Grt rim}$ , the  $T_{\text{Mg}}$  is more than  $T_{\text{Fe}}$ . Thus both three-phase fields would shift towards lower  $X_{\text{Mg}}$  side during cooling and hydration due to

reversal of the reaction (7.11) and (7.12). The shift of the three-phase fields towards Fe-rich of AFM diagram during retrogression or cooling may also be related to change in pressure conditions due to uplift during this episode.

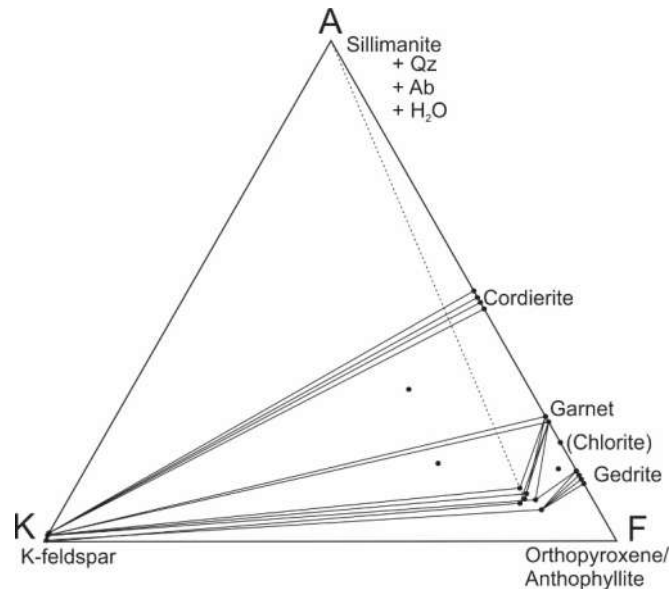


**Figure 8.4** AKF Diagrams,  $A = (Al_2O_3 + Fe_2O_3) - (K_2O + Na_2O + CaO)$ ;  $K = K_2O$ ;  $F = FeO + MnO + MgO$ , ( $A + K + F = 100$  mol%). For the pelitic granulites. Solid circles correspond to the observed mineral assemblages in the investigated area.

### 8.A.3 Petrogenetic grid

$P$ - $T$  petrogenetic grid and pseudosection can be a powerful tool for explaining phase equilibria and  $P$ - $T$  condition of a variety of bulk rock composition. The petrogenetic grid has been constructed based on Schreinmaker's analysis [416]. Each univariant reaction is designated by a bracket phase that does not participate. The  $P$ - $T$  path has schematically shown in a grid. With the updated version of the various thermodynamic dataset, a better quantitative petrogenetic grid of systems like KFMASH can be calculated and utilized to apply to natural rock system, its metamorphism [101] and for partial melting [417].  $P$ - $T$  projection or petrogenetic grid shows only the invariant and univariant equilibria and

represents the mineral equilibria information and all the reaction in a model system of the entire bulk composition variation. Reaction lines are univariant, and points are invariant, however along a univariant line the composition of a mineral phase changes continuously with the reaction leading to the appearance and disappearance of mineral phases. Although in quantitative petrogenetic grids minor components may influence the thermodynamic properties, a simple way to employ a relatively model system and characterize mineral relationship in the qualitative petrogenetic grid since only the grid's topology is considered [418]. *P-T* petrogenetic grid for KFMASH was constructed using THERMOCALC 3.21, and internally consistent thermodynamic dataset of [103]; dataset teds55, updated 2003) involving garnet (g), orthopyroxene (opx), cordierite (cd), biotite (bi), silicate melt (liq), quartz (q) and water (H<sub>2</sub>O), no bulk composition is required for the calculation of petrogenetic grid.

#### **8.A.3.1 High-grade gneiss**

A petrogenetic grid of the high-grade gneiss in FMASH system is shown in [Figure 8.5](#). The AFM diagram depicts the topology in the divariant fields. Quartz, albite, K-feldspar and water are considered as excess phases. A four-component system containing five phases, viz., garnet, gedrite, cordierite, biotite, orthopyroxene, and five univariant reactions will diverge from one invariant point. The dehydration reactions slope is calculated after the method proposed by [419]. Each univariant reaction is designated by a bracket phase that does not participate. [Figure 8.5](#) depicts that the reactions' invariant point is the thermal peak condition of the metamorphism in which the observed reactions (7.5) and (7.6) are involved as univariant reactions.



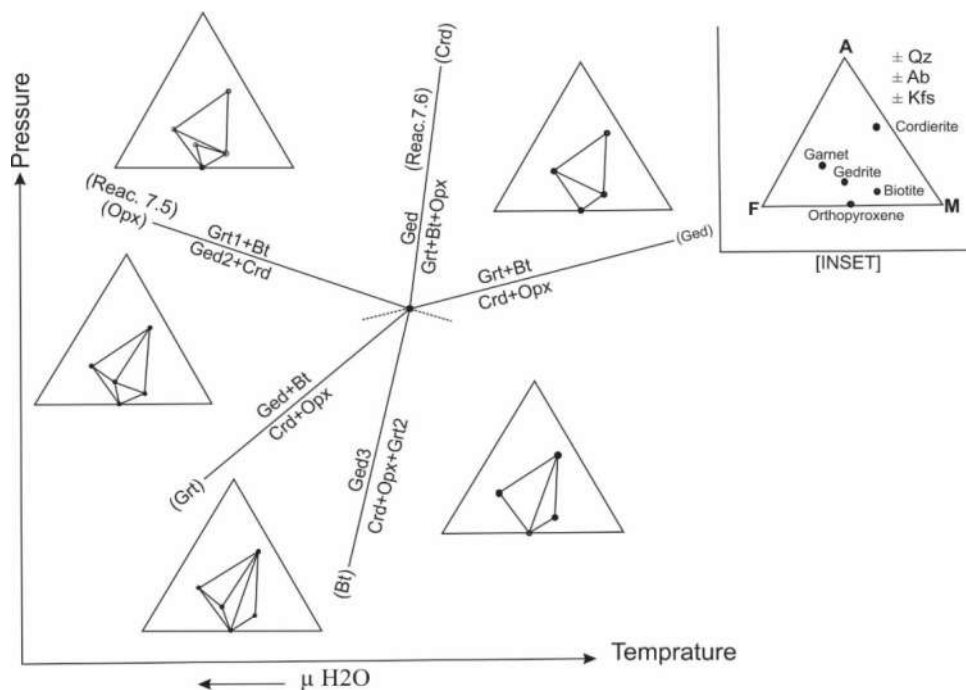


**Figure 8.5** A petrogenetic grid in the FMASH system constructed after the Schreinmakers analysis for the high-grade gneiss.

## **PART – B: Geothermobarometry**

Geothermometry and geobarometry are used for the computing temperature and pressure of metamorphic rocks, where the temperature and pressure dependencies of equilibrium constants are used as the mafic yardstick. Traditionally, the geothermobarometry has described solid-solid reactions, so that the results are independent of the partial pressure of fluid species. The primary approach for estimating the  $P$ - $T$  condition is the implementation of equilibrium thermodynamics, in which the mineral assemblages are considered to be in equilibrium, and the conditions of its formation were controlled by the  $P$ - $T$  path through which the rock has formed [420]. Values of  $\Delta H$ ,  $\Delta S$ ,  $\Delta C_p$ , and  $\Delta V$  are known from experimental calibration. The constant equilibrium value is measured for a sample using the electron microprobe analyzer (EPMA) data to determine

the elemental constituents of coexisting mineral phases. With these data, a line of “equilibrium constant” can be drawn on the  $P$ - $T$  diagram and the intersection of the two lines of “equilibrium constant” defines a unique pressure and temperature of equilibration.

### **8.B.1 Conventional geothermobarometry**

Conventional geothermobarometry involves the experimental and empirical thermodynamic calibrations of a specific reaction applied to the natural rock. This method is based on the balanced reaction between the end-member of involved mineral phases in the equilibration volume. The chemical composition of the mineral phases that may be solid solutions of various cations are calculated and the equilibrium relationships among the solid solution minerals serve as geothermometers and geobarometers. During the change in  $P$ - $T$ , the Fe-Mg exchange reaction occurs between mineral phases.

#### **8.B.1.1 Temperature estimation**

##### **8.B.1.1.a Garnet-orthopyroxene geothermometry**

Garnet and orthopyroxene coexisting in high-grade gneiss can be used to estimate the temperature in metamorphic rocks. The  $Mg^{2+}$ - $Fe^{2+}$  exchange has been proposed as a thermometer for the reaction  $3MgSiO_3 + Fe_3Al_2Si_3O_{12} \leftrightarrow 3FeSiO_3 + Mg_3Al_2Si_3O_{12}$ , which has been formulated by [82-84, 421].

##### **8.B.1.1.b Garnet-cordierite geothermometry**

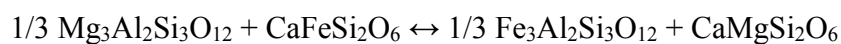
The  $P$ - $T$ - $X$  relationship among garnet and cordierite has been the subject of much debate in recent years. The geothermometer has been empirically calibrated by [86, 422]. The mixing in multi-component garnets indicates that the garnets are strongly non-ideal in the Mg-Fe binary [423, 424]. This implies that the Mg-Fe cordierites should also be non-ideal. [86, 88, 95, 425] have reformulated the geothermometer based on a thermodynamic cum statistical treatment of several pairs of naturally occurring garnet and cordierite.

#### **8.B.1.1.c Garnet-biotite geothermometry**

It is well known that the garnet-biotite geothermometer is the most widely accepted and is used to estimate the temperature equilibrium of medium grade metapelites and gneisses. Calibrations were pioneered by [426], who considered ideal solutions of these pairs. A revised geothermometry calibration has been done by [427], that takes care of many of the drawbacks of earlier calibration, including non-ideality in garnet and biotite. To have consistent data geothermometric calibrations by [86-89] have been adopted.

#### **8.B.1.1.d Garnet-clinopyroxene geothermometry**

Garnet-Clinopyroxene thermometry developed by [428] is based on the experimental Fe-Mg exchange equilibria studies. Thermometric model for the Fe-Mg exchange reaction:



The distribution coefficient function of temperature, pressure, and  $X_{\text{Ca}}$  of garnet is given by  $K_D$ , obtained from the mineral compositions. In the present calculation, the mole fraction of  $\text{Fe}^{2+}$  in the three equivalent divalent sites of garnet structure and mole fraction of Fe in cpx are considered, assuming the minerals are ideal [428].

#### **8.B.1.1.e Orthopyroxene-clinopyroxene geothermometry**

Solvus geothermometers are based on the miscibility gap in a temperature composition (T-X) space between structurally related phases. The calculation of temperature using Opx-Cpx geothermometers is formulated by calibration of the reaction between coexisting Opx and Cpx.  $[\text{Mg}_2\text{Si}_2\text{O}_6 (\text{Opx}) \leftrightarrow \text{Mg}_2\text{Si}_2\text{O}_6 (\text{cpx})]$

Several workers have experimentally and empirically studied and modelled thermometry's above reaction [429-431]. The thermometer of [429] was established on the solvus data of [432]. [430] proposed a revised model based on the calibration of a larger data set of [433,

434]. He also expressed the temperature dependence of coexisting Opx-Cpx based on the ideal solution model of [429].

### **8.B.1.2 Pressure estimation**

#### **8.B.1.2.Garnet-cordierite-sillimanite-quartz geobarometers**

The geobarometric formulations are expressed in Fe and Mg-end member equilibria. The earlier calibration for Fe end-members equilibria was based on the experimental data of [90], later experimental data of [309] were proposed which are reliable with the internally consistent dataset of [98, 101, 435]. [96, 97] calibrated barometers for garnet-cordierite-sillimanite-quartz, based on the experimental data of [309]. [96, 97] proposed an internally consistent geothermobarometer for GCAQ equilibria from which  $P$ - $T$  condition of metamorphism can be estimated simultaneously through the geobarometers plots.

#### **8.B.1.2.b Garnet-clinopyroxene-plagioclase-quartz geobarometers**

The garnet-plagioclase-clinopyroxene-quartz assemblage represents potential geobarometer. Thermodynamic calibrations for these assemblages have been formulated by [436] gives consistent results for the samples containing both pyroxenes. For the continuous reaction:  $\text{CaAl}_2\text{Si}_2\text{O}_8 + \text{Mg}_2\text{Si}_2\text{O}_6 \leftrightarrow 1/3\text{Ca}_3\text{Al}_2\text{Si}_3\text{O}_{12} + 2/3\text{Mg}_3\text{Al}_2\text{Si}_3\text{O}_{12} + \text{SiO}_2$

From the activity relations given by [436]: activities of garnet components, plagioclase activities, and diopside (cpx) activities are determined. The ideal two-site model which give good results in many applications are used here for the pyroxene components, for which the cat-ion site assignments for clinopyroxene followed here are: Ca, Na, Mn and  $\text{Fe}^{2+}$  in M2 site and  $\text{Al}^{\text{vi}}$ , Ti,  $\text{Fe}^{3+}$ , Mg and the remaining  $\text{Fe}^{2+}$  in the M1 site.

### 8.B.2 Average P-T calculation using THERMOCALC

THERMOCALC programme of [437, 438] has been used to compute the average  $P$ - $T$  using a multi-equilibrium-relationship approach to geothermobarometry. Version 3.47 has been downloaded from the website of Dr. T.J.B. Holland (2020). The computation involves calculating an independent reaction sets involving the mineral assemblage's end-members. The minerals are believed to be in equilibrium condition with each other. If there are 'n' reactions present as independent, and then also be 'n' equilibrium relationships. If the mineral compositions are known, their activities can be calculated, and hence several unknown 'n' equations are understood to characterize the metamorphic conditions. If the metamorphic fluid composition is specified, then pressure and temperature are two variables. The P-Tav is the weighted least squares procedure for calculating an ideal  $P$ - $T$  from the 'n' equilibrium relationships. Such calculations are always over-determined; a statistical process is used to calculate the unknown's best value, with more constraints than the unknown. The P-Tav involves locating the  $P$ - $T$  condition with a small displacement from the  $P$ - $T$  lines and representing equilibrium relationships [99, 100]. The  $P$ - $T$  conditions have been calculated using the  $P_{av}$ ,  $T_{av}$  and  $PT_{av}$  methods, using probe data of minerals and the THERMOCALC ver. 3.47 [99], with an internally consistent thermodynamic dataset (tc-ds62.txt) of [80] updated to comply with activity models of [169].

### 8.B.3 Application of geothermobarometers and Average PT

Accurately estimating the  $P$ - $T$  conditions is the most critical work in understanding the past or present-day lithospheric mantle's thermal state. Naturally, the reliable  $P$ - $T$  estimates can only be obtained by applying the precise and accurate geothermobarometers [439].

### **8.B.3.1 High-grade gneiss**

The PT conditions were estimated of high-grade gneisses by using the conventional garnet–orthopyroxene, garnet–biotite, garnet–cordierite exchange geothermometers and garnet–cordierite–sillimanite–quartz geobarometers, as well as sets of independent reactions between end members of mineral, were calculated by THERMOCALC v3.47 using the internally consistent data set of [99]. The estimated temperatures with garnet–orthopyroxene geothermometry for high-grade gneiss by various models are given in [table 8.1](#). The temperature lies between 788 and 869°C, and the average ‘T’ is 824±38°C. The average temperature obtained from different garnet–cordierite and garnet–biotite exchange geothermometers are at 689±12°C and 581±25°C, respectively. The avP–T condition of metamorphism for high-grade gneiss was estimated from the intersection of the different metamorphic phases involving garnet, orthopyroxene, cordierite, biotite and gedrite (with the help of THERMOCALC software), the estimated average temperature and pressure (PT<sub>av</sub>) were 7.35 kbar/792°C. The pressure calculated with the help of garnet–cordierite–sillimanite–quartz geobarometer is varies from 6.92 to 7.79 kbar.

### **8.B.3.2 Mafic granulite**

Daltonganj mafic granulite contains orthopyroxene + clinopyroxene + plagioclase as a dominant assemblage (sample KK-2). Hornblende and biotite have low availability in the rock, but their textural relationship with opx and cpx shows prograde metamorphic condition. Clinopyroxene-orthopyroxene conventional geothermometer was used to quantify temperature condition at a fixed pressure 7 kbar. The temperature of mafic granulites varied from 808 to 842°C, whereas the temperature condition of the exsolution texture of Opx-Cpx ranged from 758 and 792°C. Results of estimated *P-T* condition are

shown in Table 8.2. [431] model provided peak temperature at 842°C, whereas other models such as [429, 430], provided comparatively low temperatures. Garnet-clinopyroxene geothermometer is used to calculate temperature condition and the estimated temperature varies from 680–770°C, and garnet-clinopyroxene-plagioclase-quartz geobarometer inferred that the pressure lies between 7.78–8.25 kbar. The  $T_{av}$ ,  $P_{av}$ , and  $PT_{av}$  were estimated from different metamorphic phases, including independent reactions (THERMOCALC) among orthopyroxene, clinopyroxene, plagioclase, and amphibole end-member minerals. The  $T_{av}$  calculation was made for an assumed pressure 7 kbar with the activity of  $H_2O = 0.25$ , due to low activity of  $H_2O$  in the mineral phases. The calculated  $T_{av}$  was 821°C ( $\sigma_{fit} = 1.03$ ). However,  $P_{av}$  was calculated at 800°C temperature with the same activity of  $H_2O$ , and the calculated  $P_{av}$  was 6.84 kbar ( $\sigma_{fit} = 1.07$ ). Furthermore, the  $PT_{av}$  was calculated as 6.7 kbar/ 814°C, and  $\sigma_{fit}$  was 1.08.

### 8.B.3.3 Pelitic granulite

Garnet-biotite geothermometer was used to calculate temperature condition at a fixed pressure of 8 kbar, and the estimated temperature varies from 716 to 806°C, and garnet-biotite-plagioclase-quartz geobarometer inferred that the pressure lie at 8.47. However, garnet-cordierite geothermometer provides the temperature condition ranges from 661 to 717°C, whereas garnet-cordierite-sillimanite-quartz geobarometer was used to estimate the pressure and it ranges from 5.35 to 6.24 kbar. The  $P$ - $T$  condition results are shown in Table 8.3. The  $T_{av}$ ,  $P_{av}$ , and  $PT_{av}$  were estimated from different metamorphic phases, including independent reactions among garnet, cordierite, biotite, and plagioclase end-member minerals. The  $P_{av}$ ,  $T_{av}$  and  $PT_{av}$  calculation for peak metamorphism was  $5.85 \pm 1.86$  kbar,  $726 \pm 86^\circ\text{C}$  and  $5.94 \pm 1.7$  kbar/ $676 \pm 86^\circ\text{C}$ , respectively.

## **PART – C: Bulk Composition Modelling**

### **8.C.1 Application of equilibrium thermodynamics**

Advances in the understanding of the thermodynamic behaviour of metamorphic phases, both rock-forming and accessory constituents [98, 103, 437, 440, 441], permit the calculation of average conditions of crystallization and quantitative phase diagrams for mineral systems thought to record chemical equilibrium. This approach provides a powerful tool for establishing *P-T* paths of exhumed metamorphic rocks. To calculate geologically accurate *P-T-X* relations from metamorphic rocks, it is critical that the system's mineral phases are shown to represent a state of thermodynamic equilibrium.

Given that metamorphism is a dynamic process, with *P*, *T* and *X* changing throughout a metamorphic rock's evolution, it is uncertain whether the chemical equilibrium is a valid assumption. The kinetics of intergranular diffusion exerts a dominant control on time and length scales of metamorphic equilibration [442]. Quantitative knowledge of intergranular diffusion rates for major and trace elements remains unknown. However, an intergranular fluid phase is known to promote higher rates of elemental exchange and hence, metamorphic equilibration [443]. Accordingly, prograde (dehydration) metamorphic reactions proceed more rapidly than retrograde (hydration) reactions, accounting for the common preservation of mineral assemblages formed under peak 'T' conditions. Despite theoretical validation of the equilibrium condition, commonly observed coronal microstructures [444,445], linked segregations [446] and pseudomorphous growth structures [447] provide petrographic evidence for chemical disequilibrium, where reactions ceased prior to the total consumption of reactants. Such evidence is most commonly found in H<sub>2</sub>O under-saturated conditions and suggests sluggish



intergranular diffusion kinetics. Accordingly, it is fundamentally essential to screen samples for petrographic evidence of disequilibrium before applying equilibrium thermodynamic principles. The equilibrium model of metamorphism cannot be 'proved' in the same way as disequilibrium; instead, the absence of disequilibrium features is generally taken as supporting evidence. Furthermore, equilibrium assemblages must obey the phase rule ( $F = C + 2 - P$ , where  $F$  = variance,  $C$  = number of components, and  $P$  = number of phases present) and show consistent element partitioning between co-genetic phases.

Accepting the valid application of equilibrium thermodynamics to metamorphic rocks, thermodynamic descriptions of relevant phases [448] are combined with activity-composition models (a-x) describing the energetics of end-member phase interaction, to permit calculation of the assemblage's peak  $P$ - $T$ . Initially, this approach was limited to precisely calibrated reactions [426], followed by consideration of numerous reactions, which allowed calculation of average  $P$ - $T$  conditions [99,100,440,449]. However, such thermobarometry is limited by a dependence on mineral chemistry-inherent to the method's inverse nature. Improvements in the quality and breadth of thermodynamic data and a-x relations based on the same phase end-member compositions (internally consistent datasets – [99,101,103]), underpinned the development of forwarding phase equilibria modelling, i.e. given a reactive composition,  $P$ - $T$ ,  $P$ - $X$ , or  $T$ - $X$  relations (pseudosections) can be calculated for all phases in the system of interest.

### **8.C.2 Pseudosection modelling**

Pseudosection modelling is currently the most powerful technique employed to derive  $P$ - $T$  data from exhumed metamorphic rocks [171,450,451]. Pseudosections arose from the construction of petrogenetic grids, which show all the invariant points and

univariant lines for all phases and bulk composition in a chemical system [173,452]. Such grids provide information regarding the absolute stability of assemblages; however, they do not provide information regarding the composition and abundance of phases. Pseudosections provide a means by which the system's petrogenetic grid is modified for a specific bulk composition-effectively forming a mineral assemblage map in  $P$ - $T$ - $X$  space [171].

The validity of the pseudosection approach relies on an accurate determination of the reactive bulk composition. As discussed above, the length scales of diffusive equilibration are poorly constrained in metamorphic rocks, making this the most significant source of uncertainty inherent to the technique. Rocks containing zoned porphyroblasts are particularly challenging to model as the effective bulk composition changes with porphyroblast growth, meaning that pseudosection topology will vary as a function of time. This effect is typified by garnet's growth, which preferentially sequesters Mn during early growth stages [453]. It is possible to mitigate against reactive volume fractionation by selecting a suitable composition of garnet - i.e., from core (initiation of growth) to rim (cessation of growth) portions-to calculate the bulk composition. Pseudosections presented in this chapter are based on bulk compositions calculated from combining mineral modes unless otherwise stated.

### **8.C.3 Methodology**

The phase diagram has been calculated using the Perple\_X 6.9.0 program, which includes various sub-programs. The pseudosection is a diagram showing the various reaction conditions in the  $P$ - $T$  space, adapted to a particular bulk composition. The effective bulk rock compositions for the pseudosection calculations were obtained from the

whole-rock XRF analysis performed at the Birbal Sahni Institute of Palaeosciences (BSIP) Lucknow, India. First, the Build program has to be run containing computational option files, then the Vertex to be run in which phase diagram is calculated. Details of solution models are given in the “Perple\_X solution model glossary” and “Perple\_X Updates” ([http://www.perplex.ethz.ch/perplex\\_updates.html](http://www.perplex.ethz.ch/perplex_updates.html)). After this, the Pssect program is run that usually takes a long time to generate a postscript plot. The crude diagrams are to be finalized in any other graphic editor software. For the generation of the isopleths, the Pywerami program is employed.

#### **8.C.4 P-T Pseudosections**

##### **8.C.4.1 High-grade gneiss**

To understand how the gneiss changes different mineral assemblages when changing the metamorphic *P-T* conditions, a pseudosection have been calculated based on bulk rock composition. The NCKFMASH (Na<sub>2</sub>O-CaO-K<sub>2</sub>O-FeO-MgO-Al<sub>2</sub>O<sub>3</sub>-SiO<sub>2</sub>-H<sub>2</sub>O) system has been selected for the studied rock. The Perple\_X software (ver. 6.9.0, [78, 79]) has been used with these solid solutions: garnet, orthopyroxene, melt [103]; cordierite [417], biotite [454], amphibole [455], feldspar [103] with some pure end-member phases of quartz, and H<sub>2</sub>O included. The chemical composition of R-91-97 (in mol%; SiO<sub>2</sub> = 56.34, Al<sub>2</sub>O<sub>3</sub> = 8.77, FeO = 8.59, MgO = 14.45, CaO = 3.21, Na<sub>2</sub>O = 0.64, K<sub>2</sub>O = 1.60, H<sub>2</sub>O = 6.40) has been taken for the calculation of P-T pseudosection. MnO and TiO<sub>2</sub> contents are very low in this sample, so they are neglected from the modelling. The leucosome layer represents some liquid phases in the gneiss, and some of the H<sub>2</sub>O is present as hydrous mineral phases like; amphibole, cordierite and biotite. Amphibole (~2–3 wt% H<sub>2</sub>O), cordierite (~1–2 wt%

H<sub>2</sub>O) and biotite (~4-5wt% H<sub>2</sub>O) constitute about 10%, 20% and 10% of the total rock volume, respectively. This observation suggests ~2.5 wt% H<sub>2</sub>O for the bulk rock.

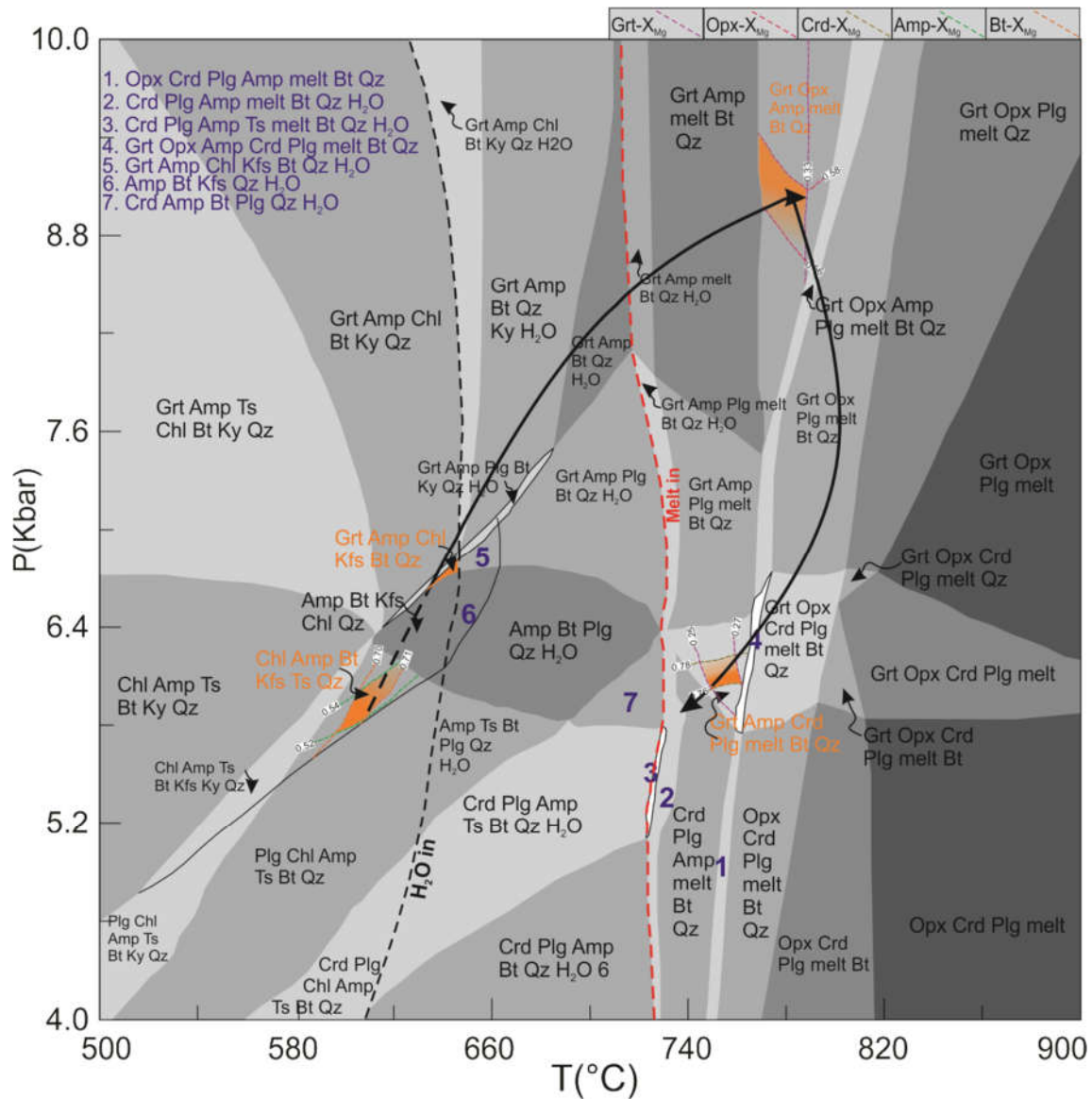


**Figure 8.6** P-T pseudosection is calculated for high-grade gneiss of sample number R-91-97 in NCKFMASH system. The mineral abbreviations are used by [279]. The  $X_{Mg}$  isopleth lines are used for garnet, orthopyroxene and cordierite.

The observed assemblages comprise garnet, orthopyroxene, amphibole, cordierite, biotite, melt, quartz, and ( $\pm$  plagioclase,  $\pm$  K-feldspar) formed at the particular  $P$ - $T$  condition. A

precise  $P$ - $T$  pseudosection has been constructed in the  $P$ - $T$  range of 4–10 kbar and 500–900 °C, with the NCKFMASH model system. The contour of isopleths of various relevant minerals such as;  $X_{Mg}$  Grt,  $X_{Mg}$  Opx,  $X_{Mg}$  Crd,  $X_{Mg}$  Amp, and  $X_{Mg}$  Bt have been calculated to define different metamorphic stages and constrain  $P$ - $T$  conditions. Here, low-grade metamorphic mineral assemblages such as Chl-Amp-Bt-Kfs-Qz suggest a primitive mineral assemblage, which further reacts to form the Grt<sub>1</sub>. The isopleths line of Amp and Bt proposes the  $P$ - $T$  condition of this assemblage ranges between 5.78–6.15 kbar and 600–622°C, and this assemblage is recognized as a pre-peak metamorphic assemblage. Here, garnet did not appear, but as the temperature increased, garnet appeared, containing a particular mineral assemblage Grt<sub>1</sub>-Chl-Amp<sub>1</sub>-Bt-Kfs-Qz. The peak metamorphic stage is characterized by the relict garnet porphyroblast (Grt<sub>2</sub>) and orthopyroxene from large relict porphyroblast that falls in the field of Grt<sub>2</sub>-Opx-Amp<sub>2</sub>-Melt-Bt-Qz (Fig.8.6). This stable mineral field shows a high range of pressure and then applies isopleth lines of Grt and Opx to  $X_{Mg}$  values that are synchronous to the mineral chemistry data. Therefore, the R-91-97 sample constrains the  $P$ - $T$  condition of the peak metamorphism at 8.65–9.42 kbar and 772–788°C (Fig.8.6). For the post-peak metamorphic stage, the mineral assemblage Grt<sub>3</sub>-Amp<sub>3</sub>-Crd-Bt-melt-Plg-Qz remains as orthopyroxene-free phase. This pseudosection field is pressure dependent, which is represented by the appearance of cordierite. Here, a large amount of Crd has evolved with Amp<sub>3</sub> around the Grt<sub>3</sub>. The Grt<sub>3</sub> and Crd are a retrograde product of Opx and Grt<sub>2</sub>, which is demarcated as the isothermal decompression (retrograde) metamorphic condition of sample R-91-97. This post-peak stage is confined at 5.71–6.18 kbar and 745–762°C, which is constrained by the isopleth lines of garnet ( $X_{Mg}$ ) and cordierite ( $X_{Mg}$ ).

#### 8.C.4.2 Mafic granulites

To investigate the  $P$ - $T$  condition of the mafic granulite (Sample KK-2), PT pseudosection was constructed in the NCKFMASHTO system ( $\text{Na}_2\text{O}$ – $\text{CaO}$ – $\text{K}_2\text{O}$ – $\text{FeO}$ – $\text{MgO}$ – $\text{Al}_2\text{O}_3$ – $\text{SiO}_2$ – $\text{H}_2\text{O}$ – $\text{TiO}_2$ – $\text{O}$ ), using Perple\_X 6.9.0 software [78, 79] and end-member thermodynamic data from [80] (filename: hp62ver.dat). The different solution models were used for various minerals like; Clinopyroxene and amphibole (G: [58]); Garnet, Orthopyroxene and Biotite (W: [169]); Plagioclase (feldspar: [456]); ilmenite (WPH: [457]), whereas quartz is taken as pure end-member. The wt% of bulk rock (sample KK-2) was normalised into mol% in the model system;  $\text{SiO}_2=49.73$ ,  $\text{TiO}_2=0.84$ ,  $\text{Al}_2\text{O}_3=8.14$ ,  $\text{FeO}=11.68$ ,  $\text{MgO}=11.57$ ,  $\text{CaO}=12.29$ ,  $\text{Na}_2\text{O}=2.14$ ,  $\text{K}_2\text{O}=0.45$ ,  $\text{H}_2\text{O} = 2.67$  and  $\text{O}_2 = 0.48$ . MnO was neglected in the model system as it was constituted only negligible amount of the total rock composition. The  $\text{O}_2$  ( $\text{Fe}_2\text{O}_3$ ) was evaluated by integrating mineral compositions and modal abundance data of the phases presented in the rock.  $\text{H}_2\text{O}$  content was recovered based on the amounts of hydrous mineral phases amphibole and biotite. Amphibole (~2-3 wt%  $\text{H}_2\text{O}$ ) and biotite (~5-6 wt%  $\text{H}_2\text{O}$ ) constituted about 15% and 5% of the total rock volume, respectively. Therefore, it was suggested that ~0.8 wt%  $\text{H}_2\text{O}$  for bulk rock composition.

The PT pseudosection of mafic granulite (sample KK-2) was shown in figure 8.7. Garnet absent assemblages was stable at low pressure, whereas orthopyroxene bearing assemblages occurred at a higher temperature. The required mineral assemblages, which are observed from petrographic analysis, was stable at PT range of >4.5 to 7.15 kbar and ~665 to 870°C. These peak mineral assemblages were best defined by the pentavariant field involving clinopyroxene, orthopyroxene, hornblende, plagioclase, biotite, ilmenite

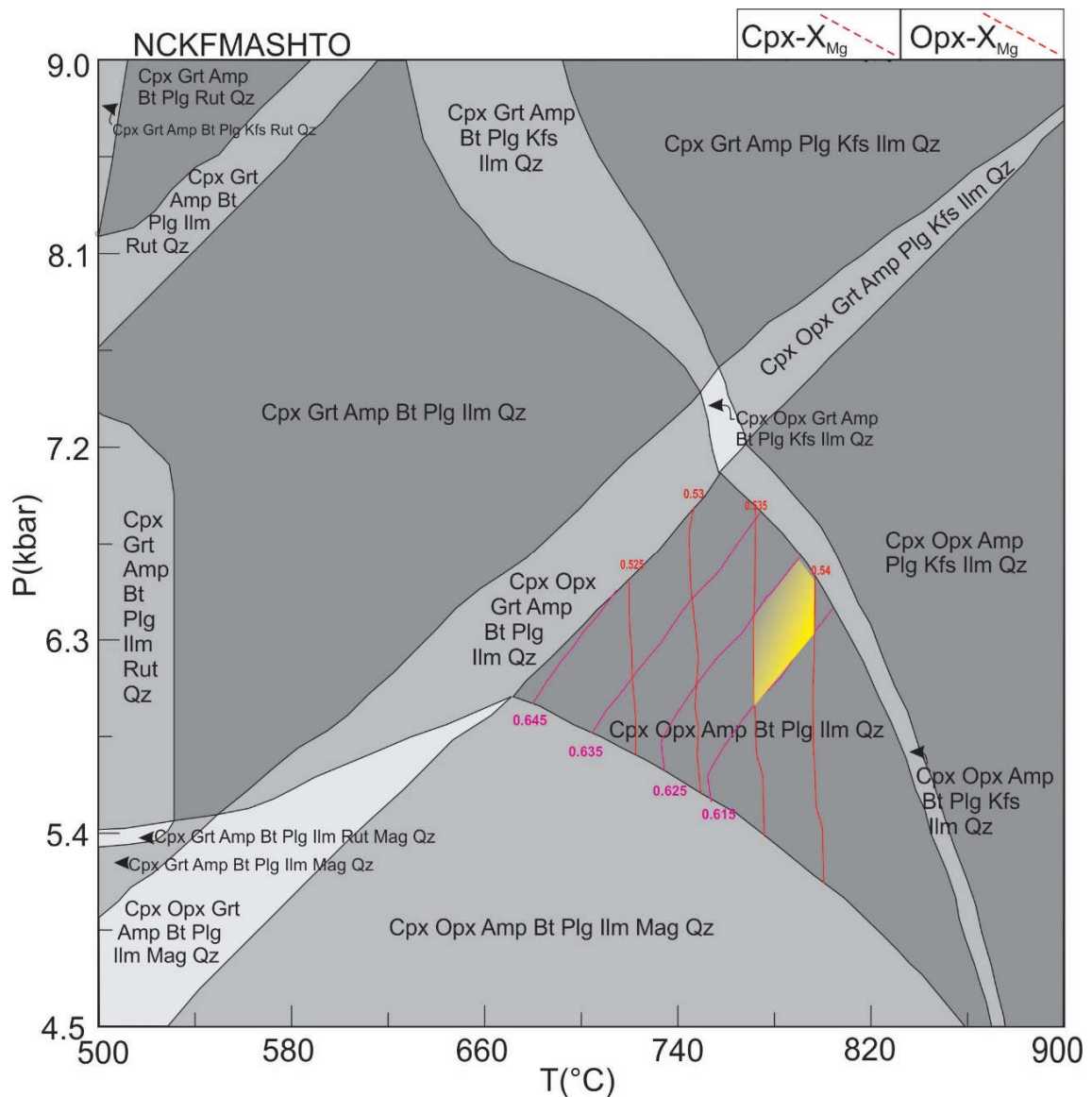


**Figure 8.7.** P-T pseudosection plot is calculated for mafic granulites from the Daltonganj in the system NCKFMASHTO. The pseudosection is contoured with isopleths of  $X_{Mg}$  of Opx and Cpx mineral assemblages. The mineral abbreviations are used by [279].

and quartz (mentioned on Fig.8.7). The P-T pseudosection for mafic granulite was contoured by  $X_{Mg}$  isopleths line of Opx and Cpx; furthermore, P-T conditions were derived by isopleth lines. The  $X_{Mg}$  value (0.535-0.540) isopleth line of orthopyroxene and 0.615-0.625  $X_{Mg}$  of clinopyroxene was demarcated as a P-T range 6.0 to 6.78 kbar pressure and temperature 775 to 808°C. This P-T range was recognized as a stable mineral phase for the

peak host assemblage. Moreover, P-T pseudosection shows magnetite-bearing fields occurring at lower temperature. Since magnetite was also observed in mineral assemblage of mafic granulites, therefore a retrograde evolution of mafic granulite has been recorded at lower temperatures (~540°C) and pressures (~4.5 kbar) within the magnetite-bearing field.

#### **8.C.4.3 Pelitic granulite**

Here, same version and model system as mafic granulites has been used for constraining the P-T pseudosection for pelitic granulites. The bulk composition of pelitic granulite (D-3) measured by XRF analysis in weight percentage, and then it converted into a mole percentage for calculating pseudosections. The sample D-3 composes; SiO<sub>2</sub>=67.83, TiO<sub>2</sub>=0.60, Al<sub>2</sub>O<sub>3</sub>=11.56, FeO=6.29, MgO=3.62, CaO=1.69, Na<sub>2</sub>O=2.54, K<sub>2</sub>O=3.34, H<sub>2</sub>O=2.00 and O<sub>2</sub> =0.52 (in mol%). There are different solution models used for the constructing the pseudosection; garnet, biotite, cordierite [169]; melt [58]; Plagioclase [456]; ilmenite [457], with some pure end-member phases aluminosilicate (sillimanite), quartz, and H<sub>2</sub>O included. The low content of the MnO in the pelitic granulite, then it is not included as a component in pseudosection calculation.

The pseudosection is characterized by large high variance (F = 3-6) garnet-bearing fields. The pre-peak metamorphic condition is defined by the cordierite, biotite and quartz crystals occur as inclusion within garnet and their respective mineral assemblages are found under low temperature and pressure conditions. The *P-T* condition of pre-peak metamorphism is found at ~3.2 kbar and ~620°C, and the *P-T* condition of this stage is derived by the X<sub>Mg</sub> isopleth contour lines of garnet and cordierite which are similar to the analyzed microprobe data. The *P-T* stability field for the peak assemblage (grt + bt + plg + sill + kfs + melt + ilm + qz) ranges from 7.40 to 9.10 kbar and 815 to 835°C. This peak



metamorphic condition has derived by the contouring of the  $X_{Mg}$  isopleths line of garnet and biotite (Figure 9). Tetravariant fields dominate the pseudosection. The assemblage is tetravariant in NCKFMASHTO and is bounded by pentavariant biotite-absent field at high-T and trivariant magnetite-bearing fields at low-P and low-T. The cordierite-in and sillimanite-out boundaries define the assemblage's under lower pressure stability. The isothermal decompression retrograde reaction has been observed from the petrographic investigation in which the consumption of garnet results in the formation of cordierite under low pressure conditions that suggest the following reaction:  $Grt + sill + qz \rightarrow crd + bt + kfs + melt$ . Garnet, biotite and sillimanite bearing assemblages are stable at higher pressure, whereas cordierite bearing assemblages dominate at the low-pressure equilibria field in the pseudosection. In the Pre-peak metamorphic stage, cordierite exists as inclusion within garnet porphyroblast with a higher  $X_{Mg}$  value of cordierite in the stable mineral assemblages, whereas retrograde metamorphic stage is characterized by cordierite present in the matrix with comparatively lower  $X_{Mg}$  values. The textural interpretation reveals that the retrograde metamorphic assemblage in  $P$ - $T$  pseudosection contains  $grt + crd + bt + plg + kfs + melt + ilm + qz + mag$ , which are stable at pressure  $\sim 4.0$  kbar and temperature  $\sim 790^\circ C$ .

**Figure 8.8** (a) (a) NCKFMASHTO  $P$ - $T$  pseudosection for pelitic granulite (D-3) showing calculated mineral equilibria for the pre-peak condition, minerals assemblage  $grt-plg-sill-kfs-bt-melt-ilm-qz$  for peak condition and retrograde metamorphism are depicted in pseudosection as  $grt + crd + bt + plg + kfs + melt + ilm + qz + mag$ , (Mineral abbreviations: [279]). (b) Isopleths for garnet, cordierite, and biotite are contoured in the  $P$ - $T$  pseudosection.  $\rightarrow$

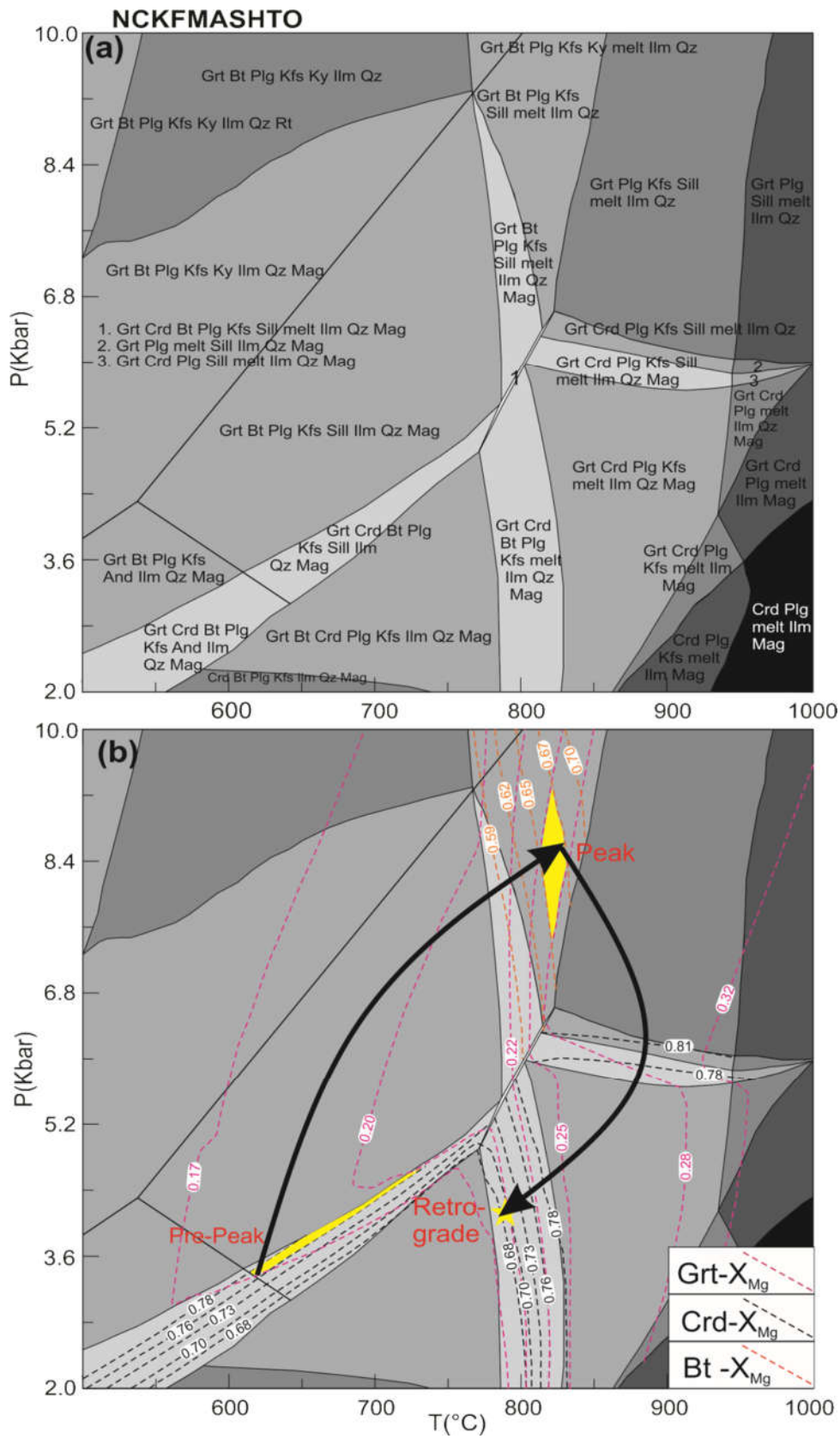


**Table 8.1a** Pressure and temperature estimates of the high-grade gniess of the study area through conventional geothermobarometers and internally consistent data set.

Estimate of Geothermometers (temp in °C) at 7 kbar						
	Grt-Opx		Grt-Crd		Grt-Bt	
	R-91-97	R-91-96	R-91-97	R-91-96	R-91-97	R-91-96
A	869	851	673	654	578	520
B	788	768	703	681	617	584
C	842	831	690	659	561	542
D	797	775	692	671	570	538
Avg.	824±38	806±41	689±12	666±12	581±25	546±27

Garnet-cordierite-sillimanite-quartz geobarometer (at 700°C)		
	R-91-97	R-91-96
a.	6.92	6.65
b.	7.79	7.43
c.	7.60	7.28
Avg.	7.43±0.46	7.12±0.41

Note: In Grt-Opx, Models of, A = [82]; B = [421]; C = [83]; D = [84] : In Grt-Crd, A = [86]; B = [88]; C = [425]; D = [95] : In Grt-Bt, A = [86]; B = [87]; C = [88]; D = [89] ; a = [86], b = [91], c = [97].

**Table 8.1b** Result of internally consistent geothermobarometry of high-grade gneiss (R-91-97) with THERMOCALC v-3.21 [103].

**(Cordierite present reaction)**

Reactions used to calculate average temperature ( $T_{av}$ ) (for $x(H_2O) = 1.0$ )			
Independent set of reaction	T in °C	Sd(T)	lnK
1) 2mgts + 3q = crd	604	166	7.671
2) 2py + 3fs = 2alm + 3en	532	455	6.990
3) 2py + 3fcrd = 2alm + 3crd	641	215	12.639
4) 3fs + 3mgts = py + 2alm	632	238	11.143
	$T_{av}$	sd	fit
Average Temp (°C)	602	47	1.01
Reactions used to calculate Average ( $P_{av}$ ) pressure (for $x(H_2O) = 1.0$ )			
	P (Kbar)	Sd (P)	lnK
5) 2py + 4alm + 9q = 6fs + 3crd	5.5	0.94	0.727
6) 2alm + en + 3q = 3fs + crd	5.9	1.11	-2.088
	$P_{av}$	sd	fit
Average Pressure in Kbar	5.56	0.93	0.61
Single end member diagnostic information of ( $PT_{av}$ )	<b>601°C/5.6 Kbar</b>		

**(Cordierite absent reaction)**

Reactions used to calculate average temperature ( $T_{av}$ ) (for $x(H_2O) = 1.0$ )			
Independent set of reaction	T in °C	Sd(T)	lnK
1) fs + fctd = alm + H <sub>2</sub> O	678	47	1.456
2) 2py + 3fs = 2alm + 3en	797	412	4.940
3) py + east = 2mgts + phl	782	427	-2.452
	$T_{av}$	sd	fit
Average Temp (°C)	752	25	0.81
Reactions used to calculate Average ( $P_{av}$ ) pressure (for $x(H_2O) = 1.0$ )			
	P (Kbar)	Sd (P)	lnK
4) alm + 2en + east = 2py + ann	7.6	12.54	-4.160
5) en + 3fs + 2east = 2alm + 2phl	7.2	4.21	5.234
	$P_{av}$	sd	fit
Average Pressure in Kbar	7.40	0.90	0.5
Single end member diagnostic information of ( $PT_{av}$ )	<b>792°C/7.35 Kbar</b>		

NOTE: where mineral abbreviations are alm = almandine, ann = annite, crd = cordierite, en = enstatite, east = eastonite, fcrd = ferro-cordierite, fs = ferrosillite, mgts = Mg-Tschermak pyroxene, q= quartz, phl = phlogopite, py = pyrope and H<sub>2</sub>O= water fluid.

**Table 8.2a** Temperature estimates of mafic granulites from conventional clinopyroxene – orthopyroxene exchange geothermometer at assumed pressure 8 kbar.

	models	KK-2	RP-2
1.	[429]	808°C	792°C
2.	[430]	828°C	814°C
3.	[431]	842°C	831°C
4.	Average	826±17°C	812±19°C

**Table 8.2b** Temperature estimates of mafic granulites (Sample: S-4) from conventional garnet – clinopyroxene exchange geothermobarometer at assumed pressure 8 kbar.

	At 8 kbar		At 800°C
A	720°C	A	8.01 kbar
B	725°C	B	7.78 kbar
C	770°C	C	8.25 kbar
D	680°C		
Avg	724±37°C	Avg	8.01±0.24

Note: In Grt-Cpx geothermometry, Models of, A = [428]; B = [458]; C = [459]; D = [460]:  
 In Grt-Cpx-Plg-Qz geobarometry, Models of, A = [461]; B = [98]; C = [462].

**Table 8.2c** Result of internally consistent geothermobarometry of (mafic granulite) orthopyroxene, clinopyroxene, plagioclase and amphibole as end-member with THERMOCALC v-3.47 [102] for sample KK-2.

(a) Reactions used to calculate <b>average temperature (T<sub>av</sub>)</b> (for x(H <sub>2</sub> O) = 0.25)						
Independent set of reaction	T in °C	Sd(T)	Sd(lnK)			
1) en + 2hed = fs + 2di	885	409	0.33			
2) en + fs + 2cats = 2mgts + 2hed	648	718	2.04			
3) 5mgts + 5hed + fact = 5fs + 5cats + tr	869	644	5.17			
4) 7fs + 10cats + 2tr = 10mgts + 14hed + 2q + 2H <sub>2</sub> O	775	374	6.29			
5) 3tr + parg = 5en + mgts + 8di + ab + 4H <sub>2</sub> O	873	56	2.11			
6) 2parg + 6q = 3en + 2di + 2jd + 2an + 2H <sub>2</sub> O	733	238	2.31			
7) 7tr + 2parg = 12en + 16di + ts + 2ab + 8H <sub>2</sub> O	837	109	8.22			
8) 2en + 2jd + 2fact = 5fs + 4di + 2ab + 2H <sub>2</sub> O	730	122	2.43			
Average Temp(°C)	T <sub>av</sub>	sd	σ fit			
	821	56	1.03			
(b) Reactions used to calculate <b>average pressure (P<sub>av</sub>)</b> (for x(H <sub>2</sub> O) = 0.25)						
Independent set of reaction	P (kbar)	Sd (P)	Sd(lnK)			
9) 5mgts + 5hed + tr + 5q = 5en + fact + 5an	6.2	5.61	5.03			
10) 4en + parg + 3an = 4mgts + 3di + jd + tr	6.8	6.12	4.14			
11) en + parg + 3an = mgts + 3cats + jd + tr	7.9	2.74	1.77			
12) mgts + parg + 4an = en + 4cats + ts + ab	6.6	7.50	7.19			
13) 2parg + 6an = 6cats + 2jd + tr + ts	5.7	5.96	7.55			
14) en + 2hed + 2parg + 6an = fs + 8cats + 2jd + 2tr	8.1	2.59	3.30			
15) 25en + 4fact + 5parg + 20an = 25mgts + 20hed + 9tr + 5ab	7.1	7.76	9.20			
16) 38cats + 6fact + 16ts + 12ab = 15fs + 12parg + 58an + 10H <sub>2</sub> O	5.6	3.82	23.27			
Average Pressure in kbar	P <sub>av</sub>	sd	σ fit			
	6.84	2.32	1.07			
(c.) Reactions used to calculate <b>average pressure and temperature (PT<sub>av</sub>)</b> (for x(H <sub>2</sub> O) = 0.25)						
Independent set of reaction						
17) mgts + di + q = en + an						
18) 4mgts + 2tr + 2q = 7en + 4an + 2H <sub>2</sub> O						
19) 5mgts + 5hed + tr + 5q = 5en + fact + 5an						
20) 2mgts + 10hed + 2tr = 5fs + 12di + 2an + 2H <sub>2</sub> O						
21) 2mgts + 4hed + ts + 4q = 2fs + tr + 4an						
22) 4en + parg + 3an = 4mgts + 3di + jd + tr						
23) 3en + parg + 4an = 3mgts + 4di + ts + ab						
24) en + parg + 3an = mgts + 3cats + jd + tr						
Single end member diagnostic information of (PT <sub>av</sub> )	Pav	Sd	Tav	Sd	Cor	σ fit
<b>6.7±1.19 kbar/814±60°C</b>	6.7 kbar	1.19	814°C	60	0.143	1.08

NOTE: where mineral abbreviations are; ab = albite, an = anorthite, cats = cassiterite, di = diopside, en = enstatite, fact = ferroactinolite, fs = ferrosilite, hed = hedenbergite, jd = jadeite, mgts = margarite, parg = pargasite, q = quartz, tr = tremolite, ts = tschermakite

**Table 8.3a** Temperature estimates of pelitic granulites from conventional geothermometry.

	Grt-Bt geothermometer (at 8 kbar)			Grt-Crd geothermometer (at 6 kbar)		
	Models	D-3	D-5	Models	D-3	D-5
1.	[86]	723°C	719°C	[86]	668°C	642°C
2.	[426]	745°C	738°C	[90]	661°C	631°C
3.	[463]	806°C	782°C	[91]	708°C	684°C
4.	[464]	762°C	764°C	[92]	682°C	661°C
5.	[87]	716°C	734°C	[93]	717°C	675°C
6.	[465]	757°C	764°C	[84]	672°C	664°C
7.	[466]	804°C	786°C	[95]	678°C	654°C
8.	Average	759±36°C	755±26°C	Average	683±21°C	658±18°C

**Table 8.3b.** Pressure estimates of pelitic granulites from conventional geobarometry.

Grt-Bt-Plg-Qz geobarometer (in kbar) (at 800°C)			
	Model	D-3	D-5
1.	[467]	8.47	7.78

Grt-Crd-Sill-Qz geobarometer (kbar) (at 600°C)			
	Models	D-3	D-5
1.	[86]	6.02	5.58
2.	[91]	6.24	6.02
3.	[96]	5.35	5.15
5.	[468]	6.11	6.12
7.	[469]	5.89	5.91
8.	[84]	5.74	5.51
9.	Average	5.89±0.32	5.71±0.37

**Table 8.3c** Result of internally consistent geothermobarometry of garnet, cordierite, biotite and plagioclase end-member with THERMOCALC v-3.33 ([103] for sample D-4.

(a) Reactions used to calculate <b>average temperature (T<sub>av</sub>)</b> (for x(H <sub>2</sub> O) = 0.5)						
Independent set of reaction	T in °C	Sd(T)	Sd(lnK)			
1) 2py + 3fcrd = 2alm + 3crd	773	155	2.61			
2) py + ann = alm + phl	658	234	2.57			
3) 5alm + 3east + 9q = 2py + 3fcrd + 3ann	726	75	0.87			
Average Temp (°C)	T <sub>av</sub> 726	sd 86	σ fit 1.12			
(b) Reactions used to calculate <b>average pressure (P<sub>av</sub>)</b> (for x(H <sub>2</sub> O) = 0.5)						
Independent set of reaction	P (kbar)	Sd (P)	Sd(lnK)			
4) 3py + 2ann + 3east + 9q = 3crd + 5phl	5.85	1.86	1.94			
Average Pressure in kbar	P <sub>av</sub> 5.85	sd 1.86	σ fit 1.94			
(c.) Reactions used to calculate <b>average pressure and temperature (PT<sub>av</sub>)</b> (for x(H <sub>2</sub> O) = 0.5)						
Independent set of reaction						
5) 2spss + 6an + 3q = 2gr + 3mncrd						
6) py + east + 3q = crd + phl						
7) py + ann = alm + phl						
Single end member diagnostic information of (PT <sub>av</sub> )	P <sub>av</sub>	Sd	T <sub>av</sub>	Sd	Cor	σ fit
<b>5.94±1.7 kbar/676±86°C</b>	5.94 kbar	1.7	676°C	86	0.56	0.82

NOTE: where mineral abbreviations are; alm = almandine, an = anorthite, ann = annite, crd = cordierite, east = eastonite, fcrd = ferro-cordierite, gr = garnet, mncrd = magnesio-cordierite, phl = phlogopite, py = pyrope, q = quartz, spss = spessartine.